The axial–radical exchange process occurring at the phosphine-substituted ruthenium atom averages the axial carbonyls d with c′ and d′ with c into two broadened resonances of equal intensity at 283 K (Table I). The two sets of radial carbonyls on the hydride-bridged rutheniums would be expected to average into two sets of two resonances each since they are also diastereotopic when axial–radial exchange is rapid at the phosphine-substituted ruthenium atom. However, only one broadened resonance is observed at 283 K, probably due to accidental overlap and broadening of the lines by the onset of axial–radial exchange at the hydride-bridged ruthenium atoms.

Experimental Section

$Ru_3(CO)_{12}$ and $HRu_3(CO)_9(-C_2$-*t*-Bu) were prepared by published procedures.[3] Deuteriodichloromethane was dried over molecular sieves (Merck). ^{13}C NMR spectra were measured on a Bruker WH-400 instrument at 100 MHz with use of a 0.1 M solution of 15–20% ^{13}CO-enriched II in CD_2C_2, 0.05 M in $Cr(acac)_3$ (Mallinckrodt). Compound II was synthesized by a procedure identical with that used for I by using $P(CH_3)(CH_2C_6H_5)(C_6H_5)$ prepared by reduction of the corresponding oxide with phenylsilane.[7] ^1H NMR (25 °C, CD_2Cl_2): δ 1.55 (9 H, s), 1.86 (3 H, d, $^2J_{^{31}P-^1H} = 11.3$ Hz), 3.51 (2 H, m), 6.68 (10 H, m), −21.1 (1 H, br). IR (KBr) ν (CO): 2075 (m), 2030 (s), 2000 (vs), 1995 (s), 1980 (s), 1940 (sh) cm^{-1}.

Acknowledgment. We gratefully acknowledge support from the donors of the Petroleum Research Fund, administered by the American Chemical Society, and the CNR of Italy (S.A.). We gratefully acknowledge the help of Dr. G. Hawkes and Dr. E. W. Randall of QMC, London, in obtaining the ^{13}C NMR data.

Registry No. II (isomer A), 93782-56-0; II (isomer B), 93861-13-3; Ru, 7440-18-8.

Contribution from the Department of Chemistry,
University of Minnesota, Minneapolis, Minnesota 55455

Synthesis and X-ray Crystal Structure of $[(dppe)_2IrAuPPh_3](BF_4)_2$

A. L. Casalnuovo, T. Laska, P. V. Nilsson, J. Olofson,
and L. H. Pignolet*

Received July 25, 1984

There has been considerable interest recently in the synthesis and structural characterization of mixed-metal cluster compounds that contain gold atoms.[1-12] Most of these clusters contain primarily carbonyl ligands bonded to the transition metals, and preparative methods have included reactions between anionic or neutral transition-metal carbonyl clusters or carbonyl hydrido clusters and monomeric gold compounds such as $Au(PR_3)Cl$ or $[Au(PR_3)]^+$. Several mixed-metal gold clusters that contain primarily phosphine ligands have been prepared by reaction of monomeric gold compounds ($AuPPh_3X$: X = Cl, NO_3) with phosphine hydrido compounds.[1,6,11] These reactions and the structures of the products have clearly shown the isolobal analogy between the hydride ligand and the $AuPR_3$ group.[8-11] See also the paper on the synthesis and structure of several new gold–iridium hydrides published in this issue of this journal.[13]

Table I. Summary of Crystal Data and Intensity Collection

Crystal Parameters	
cryst syst	monoclinic
space group	$P2_1$
cryst dimens, mm^3	0.2 × 0.3 × 0.2
cell parameters	
a, Å	11.647 (6)
b, Å	19.359 (4)
c, Å	15.952 (2)
β, deg	100.60 (2)
V, $Å^3$	3535 (3)
Z	2
d_{calcd}, g cm^{-3}	1.52
temp, °C	23
abs coeff, cm^{-1}	41.1
max, min, av transmissn factors	1.00, 0.82, 0.91
formula	$AuIrC_{70}H_{63}B_2F_8P_5$ (1)
fw	1621.9
Measurement of Intensity Data	
diffractometer	CAD 4
radiation	Mo K$\bar{\alpha}$ (λ = 0.710 69 Å) graphite monochromatized
scan type; range (2θ), deg	ω–2θ; 0–48
no. of unique reflcns measd (region)	5727 ($+h,+k,\pm l$)
no. of obsd reflcns[a]	4156 [$F_o^2 \geqslant 2\sigma(F_o^2)$]
Refinement by Full-Matrix Least Squares	
no. of parameters	424
R[b]	0.056
R_w[b]	0.070
GOF[b]	1.95
p[a]	0.04

[a] The intensity data were processed as described in: "CAD4 and SDP-PLUS User's Manual"; B. A. Frenz & Associates Inc.: College Station, TX, 1982. The net intensity $I = [K/\mathrm{NPI})](C - 2B)$, where K = 20.1166(attenuator factor), NPI = ratio of fastest possible scan rate to scan rate for the measurement, C = total count, and B = total background count. The standard deviation in the net intensity is given by $[\sigma(I)]^2 = (K/\mathrm{NPI}))^2[C + 4B + (pI)^2]$ where p is a factor used to downweight intense reflections. The observed structure factor amplitude F_o is given by $F_o = (I/Lp)^{1/2}$, where Lp = Lorentz and polarization factors. The $\sigma(I)$'s were converted to the estimated errors in the relative structure factors $\sigma(F_o)$ by $\sigma(F_o) = {}^1/_2[\sigma(I)/I]F_o$. [b] The function minimized was $\Sigma w(|F_o| - |F_c|)^2$, where $w = 1/[\sigma(F_o)]^2$. The unweighted and weighted residuals are defined as $R = (||F_o| - |F_c||)/\Sigma|F_o|$ and $R_w = [(\Sigma w(|F_o| - |F_c|))^2/(\Sigma w|F_o|)^2]^{1/2}$. The error in an observation of unit weight (GOF) is $[\Sigma w(|F_o| - |F_c|)^2/(\mathrm{NO} - \mathrm{NV})]^{1/2}$, where NO and NV are the number of observations and variables, respectively.

In this paper the synthesis of $[Ir(dppe)_2AuPPh_3](BF_4)_2$ (1) from the reaction of $[Ir(dppe)_2]BF_4$ with $AuPPh_3NO_3$ in the presence of HBF_4 in acetone solution is reported. This reaction gives some insight into the formation of the Au–Ir bond.

Experimental Section

^1H and $^{31}P\{^1H\}$ NMR spectra were recorded at 300 and 120.5 MHz, respectively, with the use of a Nicolet NT-300 spectrometer. ^{31}P chemical shifts are reported in ppm relative to the internal standard trimethyl phosphate. Solvents were dried and distilled prior to use. HBF_4 was obtained from the J. T. Baker Chemical Co. as a 48–50% aqueous solution. $AuPPh_3NO_3$[14] and $[Ir(dppe)_2]BF_4$[15] were prepared as described in the literature. All manipulations were carried out under a purified N_2

---

(1) Casalnuovo, A. L.; Pignolet, L. H.; van der Velden, J. W. A.; Bour, J. J.; Steggerda, J. J. *J. Am. Chem. Soc.* **1983**, *105*, 5957.

(2) Steggerda, J. J.; Bour, J. J.; van der Velden, J. W. A. *Recl. Trav. Chim. Pays-Bas* **1982**, *101*, 164.

(3) Mingos, D. M. P. *Proc. R. Soc. London, Ser. A.* **1982**, *308*, 75.

(4) Johnson, B. F. G.; Lewis, J.; Nicholls, J. N.; Puga, J.; Whitmire, K. H. *J. Chem. Soc., Dalton Trans.* **1983**, 787.

(5) Teo, B. K.; Keating, K. *J. Am. Chem. Soc.* **1984**, *106*, 2224.

(6) Lehner, H.; Matt, D.; Pregosin, P. S.; Venanzi, L. M. *J. Am. Chem. Soc.* **1982**, *104*, 6825.

(7) Green, M.; Orpen, A. G.; Salter, I. D.; Stone, F. G. A. *J. Chem. Soc., Chem. Commun.* **1982**, 813.

(8) Lauher, J. W.; Wald, K. *J. Am. Chem. Soc.* **1981**, *103*, 7648.

(9) Lavigne, G.; Papageorgiou, F.; F.; Bonnet, J.-J. *Inorg. Chem.* **1984**, *23*, 609 and references therein.

(10) Evans, D. G.; Mingos, D. M. P. *J. Organomet. Chem.* **1982**, *232*, 171 and references therein.

(11) Braunstein, P.; Lehner, H.; Matt, D.; Tiripicchio, A.; Tiripicchio-Camellini, M. *Angew. Chem., Int. Ed. Engl.* **1984**, *23*, 304 and references cited therein.

(12) Hutton, A. T.; Pringle, P. G.; Shaw, B. L. *Organometallics* **1983**, *2*, 1889.

(13) Casalnuovo, A. L.; Laska, T.; Nilsson, P. V.; Olofson, J.; Pignolet, L. H. *Inorg. Chem.* **1985**, *24*, companion paper in this issue.

(14) Malatesta, L.; Naldini, L.; Simonetta, G.; Cariati, F. *Coord. Chem. Rev.* **1966**, *1*, 255.

(15) Hopkinson, M. J.; Nixon, J. F. *J. Organomet. Chem.* **1978**, *148*, 201.

Table II. Table of Positional Parameters and Their Estimated Standard Deviations for 3

atom	x	y	z	B,[a] Å^2	atom	x	y	z	B,[a] Å^2
Ir	−0.37642 (8)	0.250	−0.19253 (6)	2.61 (2)	C2G	−0.530 (2)	0.344 (1)	−0.068 (2)	4.7 (6)*
Au	−0.32810 (8)	0.17864 (6)	−0.32162 (6)	3.24 (2)	C3G	−0.551 (3)	0.379 (2)	−0.007 (2)	7.4 (9)*
P1	−0.3032 (6)	0.1358 (4)	−0.4461 (4)	3.6 (2)	C4G	−0.660 (3)	0.376 (2)	0.026 (2)	7.1 (9)*
P2	−0.3636 (5)	0.1519 (3)	−0.1126 (4)	2.9 (1)	C5G	−0.748 (3)	0.333 (2)	−0.019 (2)	6.7 (8)*
P3	−0.5798 (5)	0.2409 (4)	−0.1956 (4)	3.3 (1)	C6G	−0.723 (2)	0.290 (2)	−0.087 (2)	4.9 (6)*
P4	−0.3941 (6)	0.3522 (4)	−0.2825 (5)	3.6 (2)	C1H	−0.470 (2)	0.345 (1)	−0.391 (1)	3.6 (5)*
P5	−0.1782 (6)	0.2815 (4)	−0.1748 (4)	3.4 (1)	C2H	−0.533 (2)	0.285 (1)	−0.420 (1)	3.5 (5)*
C1A	−0.448 (2)	0.111 (1)	−0.503 (2)	3.8 (5)*	C3H	−0.583 (3)	0.280 (2)	−0.504 (2)	5.4 (7)*
C2A	−0.526 (2)	0.087 (2)	−0.455 (2)	5.2 (7)*	C4H	−0.574 (3)	0.336 (2)	−0.562 (2)	6.8 (8)*
C3A	−0.646 (3)	0.068 (2)	−0.497 (2)	6.7 (8)*	C5H	−0.516 (3)	0.393 (2)	−0.538 (2)	7.5 (9)*
C4A	−0.668 (3)	0.074 (2)	−0.579 (2)	5.8 (7)*	C6H	−0.456 (3)	0.400 (2)	−0.447 (2)	5.6 (7)*
C5A	−0.599 (3)	0.094 (2)	−0.624 (2)	6.7 (8)*	C1I	−0.456 (2)	0.427 (1)	−0.244 (1)	3.6 (5)*
C6A	−0.475 (2)	0.114 (2)	−0.587 (2)	4.9 (6)*	C2I	−0.573 (3)	0.447 (2)	−0.280 (2)	5.6 (7)*
C1B	−0.242 (2)	0.194 (1)	−0.510 (1)	3.7 (5)*	C3I	−0.615 (3)	0.509 (2)	−0.242 (2)	9 (1)*
C2B	−0.173 (2)	0.174 (2)	−0.568 (2)	5.8 (7)*	C4I	0.554 (3)	0.542 (2)	0.172 (2)	9 (1)*
C3B	−0.124 (3)	0.218 (2)	−0.621 (2)	5.8 (7)*	C5I	−0.447 (3)	0.518 (2)	−0.132 (2)	8 (1)*
C4B	−0.160 (3)	0.288 (2)	−0.619 (2)	7.9 (9)*	C6I	−0.396 (3)	0.465 (2)	−0.172 (2)	5.5 (7)*
C5B	−0.236 (3)	0.311 (2)	−0.562 (2)	6.8 (8)*	C1J	−0.141 (2)	0.347 (1)	−0.088 (2)	4.2 (6)*
C6B	−0.269 (3)	0.262 (2)	−0.507 (2)	6.1 (7)*	C2J	−0.203 (3)	0.350 (2)	−0.024 (2)	7.2 (9)*
C1C	−0.213 (2)	0.059 (1)	−0.441 (2)	3.7 (5)*	C3J	−0.181 (3)	0.399 (2)	0.036 (2)	8 (1)*
C2C	−0.094 (3)	0.067 (2)	−0.406 (2)	5.4 (7)*	C4J	−0.084 (3)	0.439 (2)	0.041 (2)	7.4 (9)*
C3C	−0.015 (3)	0.011 (2)	−0.406 (2)	7.6 (9)*	C5J	−0.008 (4)	0.434 (2)	−0.013 (3)	8 (1)*
C4C	−0.065 (3)	−0.047 (2)	−0.440 (2)	8 (1)*	C6J	−0.047 (3)	0.390 (2)	−0.087 (2)	6.6 (8)*
C5C	−0.172 (3)	−0.059 (2)	−0.474 (2)	7.4 (9)*	C1K	−0.063 (2)	0.219 (1)	−0.151 (1)	3.3 (5)*
C6C	−0.254 (3)	−0.003 (2)	−0.477 (2)	5.8 (7)*	C2K	−0.025 (2)	0.200 (1)	−0.066 (2)	4.3 (6)*
C1D	−0.332 (2)	0.074 (1)	−0.168 (1)	3.3 (5)*	C3K	0.065 (3)	0.147 (2)	−0.051 (2)	5.3 (7)*
C2D	−0.411 (2)	0.025 (1)	−0.198 (2)	4.1 (6)*	C4K	0.103 (2)	0.121 (1)	−0.114 (2)	4.7 (6)*
C3D	−0.376 (3)	−0.031 (2)	−0.239 (2)	5.6 (7)*	C5K	0.068 (3)	0.137 (2)	−0.193 (2)	5.1 (7)*
C4D	−0.265 (3)	−0.042 (2)	−0.248 (2)	5.1 (7)*	C6K	−0.009 (2)	0.188 (1)	−0.215 (1)	3.7 (5)*
C5D	−0.181 (2)	0.005 (1)	−0.219 (2)	4.4 (6)*	C23	−0.512 (2)	0.134 (1)	−0.089 (1)	3.1 (5)*
C6D	−0.209 (2)	0.061 (1)	−0.181 (2)	4.6 (6)*	C32	−0.610 (2)	0.153 (1)	−0.161 (2)	3.7 (5)*
C1E	−0.278 (2)	0.148 (1)	−0.006 (1)	3.4 (5)*	C45	−0.246 (2)	0.384 (2)	−0.292 (2)	4.7 (6)*
C2E	−0.291 (3)	0.198 (2)	0.050 (2)	5.9 (7)*	C54	−0.151 (2)	0.328 (1)	−0.271 (2)	4.3 (6)*
C3E	−0.222 (3)	0.193 (2)	0.139 (2)	7.5 (9)*	B1	−0.275 (4)	0.472 (2)	0.242 (2)	6.2 (9)*
C4E	−0.158 (3)	0.143 (2)	0.157 (2)	6.4 (8)*	F1	−0.321 (2)	0.494 (1)	0.159 (2)	12.2 (8)
C5E	−0.144 (3)	0.093 (2)	0.106 (2)	7.0 (9)*	F2	−0.169 (2)	0.448 (2)	0.246 (2)	14.7 (9)
C6E	−0.206 (3)	0.091 (2)	0.027 (2)	5.6 (7)*	F3	−0.287 (3)	0.519 (1)	0.291 (2)	15 (1)
C1F	−0.699 (2)	0.255 (2)	−0.282 (1)	3.6 (4)*	F4	−0.335 (2)	0.423 (2)	0.247 (3)	22 (1)
C2F	−0.734 (2)	0.200 (1)	−0.341 (2)	4.2 (6)*	B2	0.996 (5)	0.502 (3)	0.679 (3)	10 (2)*
C3F	−0.828 (3)	0.205 (2)	−0.413 (2)	6.2 (8)*	F5	0.931 (2)	0.467 (1)	0.619 (1)	8.1 (5)
C4F	−0.893 (3)	0.266 (2)	−0.416 (2)	6.4 (8)*	F6	0.922 (2)	0.533 (2)	0.737 (2)	15 (1)
C5F	−0.867 (3)	0.320 (2)	−0.361 (2)	6.2 (7)*	F7	1.081 (3)	0.538 (1)	0.661 (2)	20 (1)
C6F	−0.767 (2)	0.312 (1)	−0.293 (1)	3.5 (5)*	F8	1.066 (3)	0.458 (2)	0.740 (2)	16 (1)
C1G	−0.614 (2)	0.296 (1)	−0.109 (2)	4.3 (6)*					

[a] Starred atoms were refined isotropically. Anisotropically refined atoms are given in the form of the isotropic equivalent thermal parameter defined as $^4/_3[a^2\beta_{1,1} + b^2\beta_{2,2} + c^2\beta_{3,3} + ab(\cos\gamma)\beta_{1,2} + ac(\cos\beta)\beta_{1,3} + bc(\cos\alpha)\beta_{2,3}]$.

atmosphere with the use of standard Schlenk techniques unless otherwise noted.

[Ir(dppe)$_2$AuPPh$_3$](BF$_4$)$_2$ (1). To a solution consisting of 100 mg (0.093 mmol) of Ir(dppe)$_2$BF$_4$ and 53 mg (0.10 mmol) of AuPPh$_3$NO$_3$ in 4 mL of acetone was added 3 μL of HBF$_4$ solution (48–50%) under constant stirring. The initially red-orange solution immediately turned to a light orange. The rapid addition of Et$_2$O resulted in the precipitation of an orange powder. Recrystallization of the orange powder from CH$_2$Cl$_2$/Et$_2$O solution afforded orange needles of **1** in 55% yield. ^{31}P{^{1}H} NMR (CH$_2$Cl$_2$, 25 °C): δ 41.4 (d, J_{P-P} = 6 Hz), −4.75 (quint, J_{P-P} = 6 Hz). Anal. Calcd for IrAuP$_5$C$_{70}$H$_{63}$B$_2$F$_8$·0.4CH$_2$Cl$_2$: C, 51.06; H, 3.89. Found: C, 50.49; H, 4.02. The presence of the CH$_2$Cl$_2$ solvate was confirmed by ^{1}H NMR, and the 0.4 composition gave the best fit to the elemental analysis.

X-ray Structure Determination. Collection and Reduction of X-ray Data. A summary of crystal and intensity data for compound **1** is presented in Table I. A crystal was secured to the end of a glass fiber with 5-min epoxy resin. The crystal class of the compound was determined by use of the Enraf-Nonius CAD 4-SDP PLUS peak search, centering, and indexing programs.[16] The intensities of three standard reflections were measured every 1.5 h of X-ray exposure time, and no decay was noted. An empirical absorption correction was applied by use of ψ-scan data and programs PSI and EAC.[16]

Solution and Refinement of the Structure. The structure was solved by conventional heavy-atom techniques. The metal atom was located by Patterson syntheses. Full-matrix least-squares refinement and difference-Fourier calculations were used to locate all remaining non-hydrogen atoms. The atomic scattering factors were taken from the usual tabulation,[17] and the effects of anomalous dispersion were included in F_c by using Cromer and Ibers'[18] values of $\Delta f'$ and $\Delta f''$. A table of observed and calculated structure factor amplitudes is avilable.[19] Hydrogen atom positions were calculated (C–H distance set at 0.95 Å) for all hydrogen atoms in the dication and were included in structure factor calculations but were not refined. Some residual electron density (1–2 e Å^{-3}) was found in a region well removed from any refined atoms. Attempts to refine carbon atom positions for peaks in this region lead to very large B values (30–40 Å^2) and unreasonable distances and angles. Although there must be partial occupancy by solvent in this region, it is so hopelessly disordered that no atoms were included. CH$_2$Cl$_2$ is suspected as this solvent since it was observed by ^{1}H NMR.

The final positional and thermal parameters of the refined atoms appear in Table II and as supplementary material.[19] The labeling scheme

---

(16) All calculations were carried out on PDP 8A and 11/34 computers with use of the Enraf-Nonius CAD4 SDP-PLUS programs. This crystallographic computing package is described by: Frenz, B. A. In "Computing in Crystallography"; Schenk, H., Olthof-Hazekamp, R., van Konigsveld, H., Bassi, G. C., Eds.; Delft University Press: Delft, Holland, 1978; pp 64–71. Frenz, B. A. In "Structure Determination Package and SDP-PLUS Users Guide"; Frenz, B. A. & Associates, Inc.: College Station, TX, 1982.

(17) Cromer, D. T.; Waber, J. T. "International Tables for X-ray Crystallography"; Kynoch Press: Birmingham, England, 1974; Vol. IV, Table 2.2.4. Cromer, D. T. *Ibid.* Table 2.3.1.

(18) Cromer, D. T.; Ibers, J. A. Reference 17.

(19) See paragraph at end of paper regarding supplementary material.

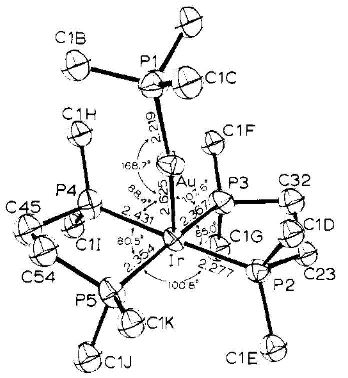

Figure 1. ORTEP drawing of the coordination core of $[Ir(dppe)_2Au(PPh_3)](BF_4)_2$ (**1**) including selected distances (Å) and angles (deg). The thermal ellipsoids show 50% probability surfaces. The esd's in Ir–Au and M–P distances and M–M–P and P–Ir–P angles are 1, 5, 1, and 2, respectively, in the last significant figure. Some additional angles (deg): Au–Ir–P2 = 89.9 (1); Au–Ir–P5 = 83.3 (1); P3–Ir–P4 = 94.2 (2); P2–Ir–P4 = 177.8 (2); P3–Ir–P5 = 167.8 (2).

is presented in Figure 1 and as supplementary material.[19]

Results and Discussion

The addition of $AuPPh_3NO_3$ to an acetone solution of $[Ir(dppe)_2]BF_4$ in the presence of HBF_4 gave a mixture of $[Ir(dppe)_2H]^{2+}$ and the binuclear complex $[Ir(dppe)_2AuPPh_3]^{2+}$ (**1**). **1** was isolated in moderate yield from this solution and was characterized by $^{31}P\{^1H\}$ NMR spectroscopy and in the solid state by a single-crystal X-ray analysis.

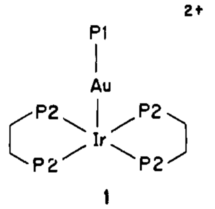

1

As shown in the drawing, **1** has an approximately square-pyramidal geometry about the IR atom. The $^{31}P\{^1H\}$ NMR spectrum is consistent with the solid-state structure and consists of a doublet and a quintet, attributable to P2 and P1, respectively: δ 41.4 (P2, d, J_{PP} = 6 Hz, intens 4), –4.75 (P1, quint, J_{PP} = 6, intens 1). No evidence for a hydride ligand was found in either the ^1H NMR or IR spectrum of **1**.

$[Ir(dppe)_2]BF_4$ was rapidly protonated in acetone solution by the addition of HBF_4 to form an equilibrium mixture of $[Ir(dppe)_2]^+$ and $[Ir(dppe)_2H]^{2+}$ as determined by ^{31}P and ^1H NMR spectroscopy.[15] The low-temperature ^1H NMR spectrum of $[Ir(dppe)_2H]^{2+}$ (–95 °C) displayed a quintet resonance at –25.5 ppm (J_{PH} = 12 Hz), also consistent with a square-pyramidal structure. It is this protonated species, apparently, that reacted with $AuPPh_3NO_3$ to form **1**. A mixture of $AuPPh_3NO_3$ and $[Ir(dppe)_2]^+$ in acetone solution, for example, did not form a detectable amount of **1**. The formation of **1** is also reversible. Addition of HBF_4 to acetone solutions of **1** generated mixtures of **1** and $[Ir(dppe)_2H]^{2+}$ as evidenced by $^{31}P\{^1H\}$ NMR spectroscopy. Thus, the proton plays a kinetic role in activating the Ir complex, a perhaps surprising result in light of the increased charge of the protonated Ir species (eq 1). Presumably, a bridged Ir–H–Au intermediate or transition state is involved in the formation of **1**.

$$[Ir(dppe)_2]^+ + H^+ \rightleftarrows [Ir(dppe)_2H]^{2+} \qquad (1)$$

$$[Ir(dppe)_2H]^{2+} + AuPPh_3NO_3 \rightleftarrows [Ir(dppe)_2AuPPh_3]^{2+} + H^+ + NO_3^-$$

The structure of **1** consists of well-separated dications and BF_4 anions. Figure 1 shows an ORTEP drawing of the $Ir(dppe)_2AuP$ core and includes atom labels and selected distances and angles. An ORTEP drawing of the entire dication and a table of all distances and angles are included as supplementary material.[19]

The geometry of the coordination core around the iridium atom is approximately square pyramidal. There are significant distortions from this idealized geometry; however, they are most likely due to a combination of nonbonded repulsions between the phenyl rings, crystal packing forces, and contraints imposed by the chelating nature of the dppe ligand. The chelate P–Ir–P "bite" angles are 85.0 (2) and 80.5 (2)° (average 82.8°) and are similar to the values found in $[Ir_3(\mu_3\text{-}AuNO_3)H_6(dppe)_3]^+$ (average 84.7 (2)°).[1] the nonchelated cis P–Ir–P angles average 97.5 (2)°, and the trans P–Ir–P angles are 177.8 (2) and 167.8 (2)°, respectively, for phosphorus atoms 2,4 and 3,5. These values show the slight distortion in the basal square plane. The dihedral angle between the IrP2P3 and IrP4P5 planes is 11°. The Ir–Au vector is approximately orthogonal to the IrP_4 basal plane (average Au–Ir–P angle is 92.3 (1)° with maximum and minimum values of 107.6 (1) and 83.3 (1)°, respectively). The Au–Ir separation (2.625 (1) Å) is short compared with values in other complexes (average 2.685 (1) Å in $[IrAu_2(H)(PPh_3)_4NO_3]BF_4$,[13] average 2.641 (1) Å in $[IrAu_3(PPh_3)_5(NO_3)]BF_4$,[1] average 2.705 (1) Å in $[Ir(\mu_3\text{-}AuNO_3)H_6(dppe)_3]^+$,[1] and 2.765 (1) Å in $[Ir(PPh_3)_3H_2(\mu\text{-}H)AuPPh_3]^+$[6]). The average Ir–P distance of 2.357 (5) Å is comparable to values found in other complexes that contain trans phosphorus atoms;[1,6] however, the Ir–P2 and Ir–P4 separations (2.277 (5) and 2.431 (5) Å) deviate significantly from the average. The large difference in the distances of these trans Ir–P bonds is unusual, but a similar phenomenon has been observed in $[Rh(dppb)_2]^+$[20] and is most likely due to nonbonded repulsions between phenyl rings. The Au–P distance in **1** (2.219 (5) Å) is short compared with values observed in other Au–Ir phosphine clusters (average 2.272 (4) Å in $[IrAu_2(H)(PPh_3)_4NO_3]BF_4$,[13] average 2.266 (4) Å in $[IrAu_3(PPh_3)_5(NO_3)]BF_4$,[1] and 2.265 (5) Å in $[Ir(PPh_3)_3H_2(\mu\text{-}H)AuPPh_3]^+$[6]).

The distances and angles within the dppe ligands and the BF_4^- anions are normal and are included as supplementary material.[19]

Acknowledgment is made to the National Science Foundation (NSF Grant CHE-81-08490) and to NATO for a travel grant. The Johnson-Matthey Co. is acknowledged for a generous loan of $IrCl_3$. We thank Professor J. J. Steggerda and his research group in Nijmegen, The Netherlands, for many helpful suggestions and discussions. A.L.C. is the recipient of an NSF Graduate Fellowship.

Registry No. $1\cdot0.4CH_2Cl_2$, 93895-64-8; $Ir(dppe)_2BF_4$, 15130-28-6; $AuPPh_3NO_3$, 14897-32-6; Au, 7440-57-5; Ir, 7439-88-5.

Supplementary Material Available: A figure of the molecular structure and tables of positional and thermal parameters, distances and angles, least-squares planes, calculated hydrogen positional parameters, and observed and calculated structure factor amplitudes (29 pages). Ordering information is given on any current masthead page.

---

(20) Anderson, M. P.; Pignolet, L. H. *Inorg. Chem.* **1981**, *20*, 4101.

Contribution from the Department of Chemistry,
Vivekananda College, Mylapore, Madras-600 004, India

Cerium(IV)-Induced Electron Transfer in Pentaamminecobalt(III) Complexes of α-Amino Acids. Evidence for the Fraction of Reaction with Synchronous N-H and C-C Bond Fissions

K. Subramani and Vangalur S. Srinivasan*

Received October 18, 1983

Studies on Ce(IV) oxidations of cobalt(III) complexes of pyridinemethanols[1] and pyridinecarboxaldehyde[2] evidenced the

---

(1) Robson, R.; Taube, H. *J. Am. Chem. Soc.* **1967**, *89*, 6487.